Oxygen and carbon isotope variations in Chamelea gallina shells: environmental influences and vital effects

Oxygen and carbon isotope variations in *Chamelea gallina* shells: environmental influences and vital effects

Arianna Mancuso[1,2], Ruth Yam[3], Fiorella Prada[4], Marco Stagioni[5], Stefano Goffredo[1,2*] and Aldo Shemesh[3]

[1] Marine Science Group, Department of Biological, Geological and Environmental Sciences, University of Bologna, Bologna, Italy

[2] Fano Marine Center, The Inter-Institute Center for Research on Marine Biodiversity, Resources and Biotechnologies, Fano, Pesaro-Urbino Italy

[3] Department of Earth and Planetary Sciences, Weizmann Institute of Science, Rehovot, Israel

[4] Environmental Biophysics and Molecular Ecology Program, Department of Marine and Coastal Sciences, Rutgers, The State University of New Jersey, New Brunswick, NJ, United States

[5] Marine Biology and Fisheries Lab, Dept. of Biological, Geological and Environmental Sciences, University of Bologna, Bologna, Italy

*corresponding author: E-mail s.goffredo@unibo.it

ABSTRACT

Stable isotopes in mollusc shells, together with variable growth rates and other geochemical properties, can register different environmental clues, including seawater temperature, salinity and primary productivity. However, the strict biological control over the construction of biominerals exerted by many calcifying organisms can constrain the use of these organisms for paleoenvironmental reconstructions. Biologically controlled calcification is responsible for the so called vital effects that cause a departure from isotopic equilibrium during shell formation, resulting in lower shell oxygen and carbon compared to the equilibrium value. We investigated shell oxygen and carbon isotopic composition of the bivalve *Chamelea gallina* in six sites along a latitudinal gradient on the Adriatic Sea (NE Mediterranean Sea). Seawater $\delta^{18}O$ and $\delta^{13}C_{DIC}$ varied from North to South, reflecting variations in seawater temperature, salinity, and chlorophyll concentration among sites. Shell $\delta^{18}O$ and $\delta^{13}C$ differed among sites and exhibited a wide range of values along the ~400 km latitudinal gradient, away from isotopic equilibrium for both isotopes. These results hampered the utilization of this bivalve as a proxy for environmental reconstructions, in spite of *C. gallina* showing promise as a warm temperature proxy. Rigorous calibration studies with a precise insight of environment and shell growth are crucial prior to considering this bivalve as a reliable paleoclimatic archive.

Keywords: bivalve; shell stable isotopes; Adriatic Sea; latitudinal gradient; vital effect

1 INTRODUCTION

Marine calcifying organisms can be considered valuable recorders of past environmental change in marine habitats (Rhoads & Lutz, 1980; Bemis *et al.*, 1998; Chauvaud *et al.*, 2005; Jones *et al.*, 2009; Schöne & Gillikin, 2013; Vihtakari *et al.*, 2017). In particular, mollusc shells are potential paleo-environmental archives due to their seasonal deposition of carbonate material, retaining high resolution temporal records of the ambient physical and chemical conditions during growth that can be detected by shell oxygen and carbon isotope composition (Klein *et al.*, 1996a; Schöne *et al.*, 2003; Purroy *et al.*, 2018).

In molluscs, calcification occurs within the extrapallial fluid (EPF), which is secreted by the mantle and is isolated from seawater (Wheeler, 1992). The composition of the EPF might be significantly altered with respect to seawater due to the influence of mantle metabolic activity or to the contribution of carbon from metabolic sources (Tanaka *et al.*, 1986; Klein *et al.*, 1996b). As a consequence of such processes, termed "vital effects" and classified as kinetic or metabolic isotope effects, biomineral compositions may depart from isotopic equilibrium. (McConnaughey, 1989a, 1989b). Thus, developmental or ontogenetic changes can obscure environmental signals, such as oxygen and carbon isotopic equilibrium fractionation, that occur in some species (McConnaughey, 1989a; Gillikin *et al.*, 2007; Schöne, 2008). Furthermore, shell growth relies on various environmental factors, including temperature, salinity and food availability, that are responsible for varying biomineralization rates and shell growth cessation when beyond the environmental optimum of the organism (Schöne, 2008; Leng & Lewis, 2016). Therefore, a detailed understanding of the physiology and growth rates of the organism that produces the mineralized structures is crucial to obtaining a reliable reading of geochemical signals from mollusc shells.

Oxygen ($\delta^{18}O$ derived from $^{18}O/^{16}O$ ratios) and carbon ($\delta^{13}C$ derived from $^{13}C/^{12}C$ ratios) isotopic composition of marine mollusc carbonates are robust proxies for seawater

69 temperature and dissolved inorganic carbon, respectively (Krantz *et al.*, 1987; Bemis & Geary,

70 1996; Hickson *et al.*, 1999; Goodwin *et al.*, 2001; Elliot *et al.*, 2003). Shell oxygen isotope

71 composition ($\delta^{18}O_{shell}$) is a function of temperature, salinity and the oxygen isotope composition

72 of seawater ($\delta^{18}O_{sw}$) at the time of precipitation (Epstein & Mayeda, 1953; Craig, 1965). The

73 temperature dependence of $\delta^{18}O$ fractionation in biogenic carbonates has been linked to

74 species-specific vital effects (Wefer & Berger, 1991; Bemis *et al.*, 1998; Böhm *et al.*, 2000). Shell

75 carbon isotope composition ($\delta^{13}C_{shell}$) is determined by the isotopic composition of the

76 dissolved inorganic carbon in seawater ($\delta^{13}C_{DIC}$) and by the proportion of metabolic carbon

77 involved in the calcite/aragonite precipitation (Sadler *et al.*, 2012). The amount of metabolic

78 respiratory CO_2 incorporated into the skeleton is species-dependent, varying from less than

79 10% to over 35%, and it can be high enough to overshadow the $\delta^{13}C_{DIC}$ signal (Klein *et al.*,

80 1996b; Lorrain *et al.*, 2004; Gillikin *et al.*, 2005, 2006).

81   While the incorporation of respired CO_2 within the body of an organism is linked to

82 metabolic effects (McConnaughey *et al.*, 1997), kinetic effects are specifically associated with

83 processes such as shell crystal growth rate, hydration and hydroxylation of CO_2 in solution

84 (McConnaughey, 1989b) and the isotope fractionation between species of $\delta^{13}C_{DIC}$ which are

85 present in the calcifying fluids (Spero *et al.*, 1997; Zeebe, 1999; Adkins *et al.*, 2003; Tripati *et*

86 *al.*, 2010). Taking into account the amplitude of the biologically induced fractionation, in

87 addition to environmental conditions, is crucial for a reliable interpretation of $\delta^{18}O$ and $\delta^{13}C$

88 signatures from molluscs specimens.

89   The present study aimed to investigate shell $\delta^{18}O$ and $\delta^{13}C$ in the clam *Chamelea gallina*

90 along a latitudinal gradient in the Adriatic Sea (~400km). Shell isotopic profiles of *C. gallina*

91 were also investigated to study ontogenetic variations in shell $\delta^{18}O$ and $\delta^{13}C$ along the gradient.

92 This study also monitored seawater $\delta^{18}O$ and $\delta^{13}C_{DIC}$ along the Adriatic Sea latitudinal gradient,

93 where the presence of Po river delta plays a crucial role in the biogeochemical processes of this

4

basin. The Po is the largest Italian river in terms of both length (652 km long) and average discharge (1,500 m³ s⁻¹; Montanari, 2012), supplying over 50% of freshwater input to the Northern Adriatic basin (Degobbis *et al.*, 1986) and about 20% of total river discharge in the Mediterranean Sea (Russo & Artegiani, 1996). Fluvial $\delta^{13}C_{DIC}$ has usually lower isotopic composition than oceanic due to the presence of CO_2 originated from the decomposition of terrestrial vegetation (McConnaughey & Gillikin, 2008). In the Po Plain-Adriatic Sea system, a strong geomorphological change took place during the Holocene in response to the glacio-eustatic sea-level variations (Amorosi *et al.*, 2019). In the past, the North Western Adriatic coastal area was characterized by estuary systems, bounded seaward by a series of sandbars that isolated coastal lagoons and limited riverine plumes into the Adriatic (Amorosi *et al.*, 2019). This past more stable shoreface depositional setting due to reduced influence of riverine plumes, warmer temperature and higher aragonite saturation state than today seemed to reduce the thermodynamic work required for organisms to deposit calcium carbonate (Hall-Spencer & Harvey, 2019), making the calcification less expensive in terms of metabolic cost (Clarke, 1993; Cheli *et al.*, 2021). Nowadays, the western Adriatic basin is characterized by the northern area with shallow continental shelf, representing the result of several southward progradations driven by sea level cycles, by the central Adriatic Sea, a small remnant basin reaching 260 m water depth and confined to the north by the Po River delta formed during the last sea level lowstand and by the Southern Adriatic Sea, originated as a consequence of the interaction between mass transport processes and deep water circulation (Ridente *et al.*, 2007, 2008). The Adriatic Sea is a dynamic environment influenced by terrestrial, atmospheric and oceanic processes that provide many challenges to understanding these systems (Canuel *et al.*, 2012; Pérez *et al.*, 2016). In addition to environmental drivers such as freshwater discharge and coastal upwelling, it can be impacted, as the other coastal zones, by increases in atmospheric pCO₂ with the alteration of the distribution of reactive inorganic carbon species,

119 thus reducing pH values and the saturation state for calcium carbonate minerals (Ω) (Feely *et*

120 *al.*, 2004; Gazeau *et al.*, 2007; Harris *et al.*, 2013; Pérez *et al.*, 2016) and anthropogenic change

121 of river basins that further influence the natural export of water, nutrients, and carbon to

122 estuarine and coastal marine ecosystems (Regnier *et al.*, 2013; Pérez *et al.*, 2016). The

123 carbonate chemistry of riverine-influenced near shore environments is therefore affected by

124 lower salinity and resultant decreased alkalinity, eutrophication and resultant

125 production/respiration cycles (Salisbury *et al.*, 2008; Pérez *et al.*, 2016).

126   This study covers several sites along the latitudinal gradient in the Adriatic Sea and will

127 contribute to the understanding whether vital/ontogenic process or environmental conditions

128 govern the shell isotopic signature in the bivalve *C. gallina*, giving insight into the use of bivalve

129 archives as providers of environmental information.

130

131

132 **2 MATERIALS AND METHODS**

133

134 **2.1 Sample collection and treatment**

135 Specimens of *C. gallina* were collected from six sites in the Western Adriatic Sea from 45°42′N

136 to 41°55′N, spanning ~400 km of latitudinal gradient, ~2°C of average sea surface temperature,

137 ~9 PSU of average sea surface salinity and ~5 mg/m³ of average chlorophyll concentration

138 (Fig. 1-2). Because of the shallow sampling conditions (not beyond 5 meters of water depth)

139 and the well mixed water column we assume homogeneous environmental parameters

140 between surface and bottom.

141   Clams were sampled using hydraulic dredges at 3–5 m depth on sandy or mud bottoms

142 along the Eastern Italian coasts in six sites from North to South (Fig. 1), Monfalcone (MO),

143 Chioggia (CH), Goro (GO), Cesenatico (CE), San Benedetto (SB) and Capoiale (CA). Seawater

6

144   samples were collected in the six sites in summer (August) and winter (February) in duplicate.

145   In August and February, seawater was the warmest and coldest of the year, respectively, with

146   no sharp shifts in salinity, as occurred during autumn and spring in response to increases

147   rainfall and corresponding river discharge. Although two seawater samples did not allow the

148   capture of seasonal variability over months and years, they can indicate annual seawater

149   isotopes extremes. Seawater samples were stored in plastic jars of 100 ml without additional

150   treatments for $\delta^{18}O$ and in glass bottles with 1 ml of saturated mercuric chloride ($HgCl_2$) for

151   $\delta^{13}C_{DIC}$, in order to stop all biological activity.

2.2 Oxygen and carbon isotopic compositions

154   For shell $\delta^{18}O$ and $\delta^{13}C$ analysis, 7-8 shells from each site were selected and treated with a

155   solution of H_2O_2 (10% buffered with ammonium hydroxide) to clean the surface from

156   exogenous sources of oxygen and carbon. Shell powders were manually collected by means of

157   a dental drill (0.5 mm diameter) on the shell surface. The isotope ratios of the shells were

158   determined by using "average shell powder", which is the combined powders drilled in several

159   points along the shell growth axis (Fig. S1). Seasonal $\delta^{18}O$ and $\delta^{13}C$ profiles were carried out on

160   one shell from each of the five sites, by drilling "spot" samples in sequence from the umbo

161   (oldest zone of the shell) to the ventral edge (youngest zone) along the shell growth axis with

162   ~1.4 mm mean spatial resolution. The necessity of roasting to pyrolise the organic matter

163   before isotopes analyses (350°C for 45 min in vacuo; Keller *et al.*, 2002) was tested by analyzing

164   12 random powder samples taken from all sites. Shell $CaCO_3$ samples of 180-250 µg of powder

165   were flushed with helium gas and reacted with 100% orthophosphoric acid (H_3PO_4) and left to

166   equilibrate at 25°C for 24h. The evolved CO_2 gas was analyzed using a Finnigan GasBench II

167   connected in line to a Finnigan MAT252 isotope ratio mass spectrometer at the Department of

168   Earth and Planetary Sciences, Weizmann Institute of Science. The shell $\delta^{18}O$ and $\delta^{13}C$ data are

169   reported against VPDB-standard.

170   The analysis of seawater oxygen isotope ($\delta^{18}O_{sw}$) was performed by mixing 0.5 ml of

171   seawater with 0.5% CO_2 in helium at 25°C for 24h. The values are reported in per-mill relative

172   to the Vienna Standard Mean Ocean Water (VSMOW; ±0.05‰ long-term precision of

173   laboratory). For carbon isotopes analysis of seawater ($\delta^{13}C_{DIC}$), 1 ml of seawater was injected

174   into gas vials pre-flushed with helium and left to react with 0.15 ml H_3PO_4 at 25°C for 24h. The

175   results are reported relative to the international Vienna-PeeDee Belemnite standard (VPDB;

176   ±0.08‰ long-term precision of $NaHCO_3$ laboratory standard).

177   SST in each site were reconstructed from shell isotopic composition along the growth

178   axis and $\delta^{18}O_{sw}$ to compare with SST data from satellite, by using the equation from Grossman

179   & Ku, 1986 [$T = 20.6 - 4.34(\delta^{18}O_{arag} - (\delta^{18}O_{sw} - 0.27))$] (Bemis *et al.*, 1998). In particular, SST

180   were estimated from seasonal $\delta^{18}O_{shell}$ profile corrected with measured $\delta^{18}O_{sw}$ (winter, summer

181   and average values for each sites) and with calculated $\delta^{18}O_{sw}$ reconstructed from salinity data

182   (winter, summer and average sea surface salinity for each sites), using the equation derived

183   from Purroy *et al.*, 2018 for the coastal areas in the eastern Adriatic Sea [$\delta^{18}O_{sw} = 0.23$ x salinity

184   - 7.54]. The estimated SSTs were temporally aligned with satellite data, starting from the shell

185   ventral margin corresponding to time of sampling, and backwards sinusoidal sequence of

186      $\delta^{18}O_{shell}$ defined the seasonal values to consider in the equations (winter for higher peaks,

187   summer for lower peaks and average values for intermediate points).

188

189   **2.3 Diffractometric measurements**

190   XRD analyses were carried out in one specimen for each site to determine shell mineral phases.

191   Diffraction patterns were obtained by means of a D2 Phaser diffractometer with Lynxeye

192   detector, using Cu-Kα radiation generated at 30 kV and 10 mA at the department of Earth and

193   Planetary Sciences in Weizmann Institute of Science. XRD patterns were analyzed using the

194   Diffract.Eva software.

195

196   **2.4 Shell growth parameters**

197   Clam shell length (L, maximum length on the anterior-posterior axis), was calculated with

198   ImageJ software after capturing shell shape with a scanner. Annual growth rates were

199   calculated with the length/age ratio, by using the age obtained from $\delta^{18}O$ profile along the shell

200   growth axis.

201

202   **2.5 Environmental parameters**

203   For each site, sea surface temperature (SST; °C) and sea surface salinity (SSS; PSU) data were

204   extrapolated from the database of the Euro-Mediterranean Center on Climate Change. The

205   annual average of SST and SSS were obtained from daily values from July 2011 to July 2015,

206   while chlorophyll concentration (CHL; mg/m^3) was calculated from monthly values from the

207   *GlobColour data* by ACRI-ST, France. The selected range of four years for the environmental

208   parameters ensured to enclose the full lifespan of *C. gallina*, reported to be of two-three years

209   in the Adriatic Sea (Mancuso *et al.*, 2019).

210

211   **2.6 Statistical analyses**

212   Significant differences of SST, SSS, CHL, $\delta^{18}O_{sw}$, $\delta^{13}C_{DIC}$ and shell $\delta^{18}O$ and $\delta^{13}C$ among sites were

213   tested with the one-way analysis of variance (ANOVA). The non-parametric Kruskal-Wallis

214   rank test was used when assumptions for parametric statistics were not fulfilled. The

215   correlations between $\delta^{18}O_{sw}$ and $\delta^{13}C_{DIC}$ with latitude were calculated with Spearman's rank

216   correlation coefficient (r_S). A General Additive Model (GAM; package mgcv) was used to analyze

217   the influence of different environmental factors on shell $\delta^{18}O$ and $\delta^{13}C$ data. GAM are non-

218   parametric regression techniques that are not restricted by linear relationships, thus they

219   provide a flexible method for analysis when the relationship between variables is complex.

220   GAM was selected based on the gain in deviance explained (%) and on the reduction in Akaike's

221   information criterion (AIC) and generalized cross validation score (GCV) compared to linear

222   model (Table S1). All data analyses were computed using RStudio Software(RStudio Team,

223   2020).

224

225

226   **3 RESULTS**

227

228   **3.1 Environmental parameters, $\delta^{18}O_{sw}$ and $\delta^{13}C_{DIC}$**

229   SST, SSS and CHL from satellite were significantly different among sites in the Adriatic Sea

230   (Kruskal-Wallis test, p<0.001; Fig. 1-2). SST and SSS correlated negatively with latitude, while

231   CHL showed the opposite trend.

232   Summer, winter and annual mean $\delta^{18}O_{sw}$ and $\delta^{13}C_{DIC}$ were significantly different among

233   sites (Kruskal-Wallis test, p<0.001, Table 1) and correlated negatively with latitude, except for

234     $\delta^{13}C_{DIC}$ in summer (Fig. 3). $\delta^{18}O_{sw}$ showed positive values while in Chioggia and Goro the $\delta^{18}O_{sw}$

235   shifted sharply towards negative values in summer (-1.24‰ and -2.84‰, respectively), even

236   lower than the values in winter (Table 1; Fig 3). In winter, negative $\delta^{18}O_{sw}$ values were still

237   found in Goro (-0.65‰), together with Cesenatico (-0.60‰) and the resulting annual mean

238     $\delta^{18}O_{sw}$ showed considerably lower values in Goro (-1.75‰) and marginally lower in Chioggia

239   and Cesenatico (-0.19‰ and -0.06‰, respectively; Table 1; Fig 3). Goro stood out for its deeply

240   low values of $\delta^{13}C_{DIC}$ in both seasons (-3.54‰ in summer and -2.34‰ in winter), while Capoiale

241   was the only site with positive value of $\delta^{13}C_{DIC}$, both in summer and winter season (0.28‰ and

242   0.11‰, respectively; Table 1; Fig 3).

243   Using the annual mean temperature from all sites along the latitudinal gradient

244   (17.25°C), the estimated isotopic value for biological aragonite deposited in equilibrium with

245   ambient seawater {calculated from Grossman and Ku, 1986 for oxygen [$T = 20.6 - 4.34(\delta^{18}O_{arag}$

246     $- (\delta^{18}O_{sw} - 0.27))$] and Romanek et al., 1992 for carbon ($\delta^{13}C_{arag} = \delta^{13}C_{DIC} + 2.7$)}, resulted in

247   0.77‰ +/- 0.25‰ for $\delta^{18}O$ and 2.70‰ for $\delta^{13}C$ (Fig. 4). $\delta^{18}O_{sw}$ and $\delta^{13}C_{DIC}$ were not included

248   in the equation as the graph axis are, $\delta^{18}O_{shell} - \delta^{18}O_{sw}$ and $\delta^{13}C_{shell} - \delta^{13}C_{DIC}$, respectively.

249

250   **3.2 Shell $\delta^{18}O$ and $\delta^{13}C$**

251   CaCO$_3$ of the analyzed shells of *C. gallina* consisted of aragonite as indicated by XRD patterns

252   obtained for six specimens (one specimen per site; Fig. 5). The roasting test showed no

253   differences in the $\delta^{18}O_{shell}$ and $\delta^{13}C_{shell}$ between roasted and not roasted powders, with a

254   homogeneous distribution of values obtained from the two procedures ($p > 0.05$;

255   Supplementary Fig. S2). Hence, additional roasting treatment was avoided.

256     $\delta^{18}O_{shell}$ and $\delta^{13}C_{shell}$ were different among sites (Kruskal-Wallis test, $p < 0.001$; Table 2).

257   In order to consider the isotopic composition of the local seawater, shell isotope data were

258   corrected with annual mean $\delta^{18}O_{sw}$ and $\delta^{13}C_{DIC}$ of each site and the corrected data (indicated as

259     $\delta^{18}O_{shell} - \delta^{18}O_{sw}$ and $\delta^{13}C_{shell} - \delta^{13}C_{DIC}$) were still different among sites (Kruskal-Wallis test,

260     $p < 0.001$; Table 2). A strong positive correlation between $\delta^{18}O_{shell} - \delta^{18}O_{sw}$ and $\delta^{13}C_{shell} - \delta^{13}C_{DIC}$

261   was observed considering the entire isotope dataset ($p < 0.001$; Fig. 4). The measured isotopic

262   values were far from the mean annual estimated aragonite equilibrium value (0.77‰; Fig. 4).

263   Only Goro, clustered away from the other sites for both $\delta^{18}O_{shell} - \delta^{18}O_{sw}$ and $\delta^{13}C_{shell} - \delta^{13}C_{DIC}$,

264   showing $\delta^{18}O_{shell} - \delta^{18}O_{sw}$ values close to the aragonite equilibrium value (Fig. 4). Moreover, only

265   Goro showed positive $\delta^{18}O_{shell} - \delta^{18}O_{sw}$ values, while San Benedetto and Capoiale, the warmer

266   sites, showed lower values (Table 2; Fig. 4). $\delta^{18}O_{shell} - \delta^{18}O_{sw}$ showed a slight positive correlation

267   with latitude ($p < 0.05$; Table S2; Fig. 6), due to higher values reported at Goro (0.76‰), while

11

the two Northern sites, Monfalcone and Chioggia, had lower values (Table 2; Fig. 6). $\delta^{18}O_{shell}$ - $\delta^{18}O_{sw}$ was also correlated with SST and SSS ($p < 0.001$; Table S2; Fig. 6) and with chlorophyll ($p < 0.05$; Table S2; Fig. 6).

$\delta^{13}C_{shell}$ - $\delta^{13}C_{DIC}$ showed no correlation with latitude (Table S2), despite the similar pattern of $\delta^{18}O_{shell}$ - $\delta^{18}O_{sw}$, with Goro that presented the highest values (Table 2-S2). SST, SSS and CHL showed significant correlations with shell $\delta^{13}C_{shell}$ - $\delta^{13}C_{DIC}$ among the six sites ($p < 0.01$ for SST and $p < 0.001$ for SSS and CHL; Table S2; Fig. 6).

Seasonal analysis obtained from the drilled spots along a single shell growth axis revealed that the drilling method, with a mean spatial resolution of $\sim$1.4 mm, resulted in a sinusoidal sequence of lighter and heavier $\delta^{18}O_{shell}$ with the detection of distinctive seasonal peaks in the $\delta^{18}O_{shell}$ - $\delta^{18}O_{sw}$ (Fig. 7). The age of five specimens could be defined by counting the sequence of summers (lighter values) and winters (heavier values), and the reduction of the growth rates could be detected with increasing age by the reduction of width of sinusoidal sequences (Fig. 7). The shells from Monfalcone and Goro were probably born at the end of summer, while the shells from the other sites were born early in spring or at the beginning of summer, according with the first $\delta^{18}O_{shell}$ values in each curve (Fig. 7).

SST derived from measured $\delta^{18}O_{shell}$ and $\delta^{18}O_{sw}$ reflected the SST from satellite during warm seasons in all sites except in Goro, where only SST calculated with $\delta^{18}O_{sw}$ predicted from summer salinity data aligned with summer SST from satellite (Fig. 8). In the cold season SST derived from both measured $\delta^{18}O_{sw}$ and predicted $\delta^{18}O_{sw}$ from salinity seemed to overestimate the temperature in all sites (Fig. 8). In Goro, reconstructed SST from $\delta^{18}O_{sw}$ results are inconsistent with winter seasonal peaks (Fig. 8). In general, the two methods used for obtaining SST from measured $\delta^{18}O_{sw}$ and from predicted $\delta^{18}O_{sw}$ from salinity agree, showing similar SST in five sites, except in Goro (Fig. 8). In Goro, SST derived from measured $\delta^{18}O_{sw}$ showed no

292   seasonal profile, suggesting an apparent uncertainty in the measured $\delta^{18}O_{sw}$ values in this site

293   (Fig. 8).

294       $\delta^{13}C_{shell}$ - $\delta^{13}C_{DIC}$ of *C. gallina* differed within the shells and among sites, showing a

295   decreasing trend from the umbo to the ventral edge in all shells and higher variability for

296   $\delta^{13}C_{shell}$ - $\delta^{13}C_{DIC}$ in the shells from the Northern sites (Fig. 7). The large variability in $\delta^{13}C_{shell}$ -

297   $\delta^{13}C_{DIC}$ was observed especially over 30 mm in the shells of Goro and Cesenatico, where

298   considerable peaks of reduced $\delta^{13}C_{shell}$ - $\delta^{13}C_{DIC}$ were depicted (-4.17‰ and -3.91‰

299   respectively; Fig. 7). Positive correlation was found between shell carbon isotope values and

300   annual growth rate (Fig. 9).

301

302

303   **4 DISCUSSION**

304

305   Shell $\delta^{18}O$ and $\delta^{13}C$ of the clam *C. gallina* and seawater oxygen and carbon isotope signatures

306   were investigated for the first time under varying temperature, salinity, and chlorophyll

307   concentration conditions along a wide latitudinal gradient in the Adriatic Sea. The Po river

308   inflows in the Northern Adriatic Sea and heavily modifies salinity and chlorophyll

309   concentrations from North to South (Gilmartin *et al.*, 1990; Catalano *et al.*, 2014). Po river is

310   responsible for 50% of the total nutrient input (Pettine *et al.*, 1998), that gives rise to

311   phytoplankton blooms in spring, making the Northern Adriatic Sea the area with the highest

312   average primary production in the Adriatic basin (588g C m^2 y^1; Gilmartin *et al.*, 1990). In

313   contrast, in the Middle and Southern Adriatic Sea primary production is significantly lower

314   (137 and 97g C m^2 y^1, respectively), resulting in a relevant eutrophic/oligotrophic gradient

315   along the Eastern coasts of Italy from North to South (Giordani *et al.*, 2002).

The biology of the clam *C. gallina* in the Adriatic Sea was already studied in terms of growth

rate (Keller *et al.*, 2002; Mancuso *et al.*, 2019; Bargione *et al.*, 2020), physiology (Matozzo *et al.*,

2007; Monari *et al.*, 2007a, 2007b), and shell properties (Gizzi *et al.*, 2016; Mancuso *et al.*, 2019;

Cheli *et al.*, 2021). A previous study conducted in the Bay of Trieste in the North of the Adriatic

Sea investigated the shell isotopic composition of *C. gallina* in relation to its growth rates and

settlement time (Keller *et al.*, 2002). However, this confined area is not representative of the

wide shifts in *C. gallina* habitat from North to South of the Adriatic basin that influence shell

growth (Mancuso *et al.*, 2019).

4.1 $\delta^{18}O_{sw}$ and $\delta^{13}C_{DIC}$

In this study, both $\delta^{18}O_{sw}$ and $\delta^{13}C_{DIC}$ varied along the ~400 km transect in the Adriatic Sea. The

annual $\delta^{18}O_{sw}$ varied by 3.27‰ VSMOW along the latitudinal gradient, in contrast to the

remarkably constant $\delta^{18}O_{sw}$ along the 850 km North-South transect in the Italian Western coast

(0.65‰ ± 0.23 SD; Prada *et al.*, 2019). The main driver controlling $\delta^{18}O_{sw}$ in this region is the

increase of freshwater inflows and the large salinity changes, from ca. 29 to 37 PSU, from the

area around the Po delta towards the South. Freshwater mixing from the Po river ($\delta^{18}O$ close

to -10‰; Bortolami *et al.*, 1973) leads to low salinity conditions (< 30 PSU) and extremely low

$\delta^{18}O_{sw}$ values (-1.75‰) in Goro. The Po is dominated by two annual floods due to raised rainfall

in autumn and snow-melt in spring (Flora & Longinelli, 1989; Tesi *et al.*, 2007) and largest

minimum, largest average and largest maximum daily river flow are observed to be 275 m^3 s^{-1},

1470 m^3 s^{-1} and 10 300 m^3 s^{-1}, respectively (Montanari, 2012). The freshwater gain along the

coastline of the Northern basins results in a negative difference between the freshwater losses

by evaporation and the gains by runoff and precipitation, making the Adriatic Sea a dilution

basin compared to the Mediterranean Sea as a whole (Raicich, 1996). Moreover, the surface

circulation of the Adriatic Sea is primarily thermohaline, driven by dense water formation

341 related to the surface heat losses: cool and with low salinity North Adriatic dense Deep Water

342 (NAdDW), that flows southwards and Southern Adriatic dense Deep Water (SAdDW), favoured

343 by cyclonic gyre (Russo & Artegiani, 1996; Zavatarelli *et al.*, 1998). Positive $\delta^{18}O_{sw}$ values were

344 reported in the Southern sites (1.52‰ in Capoiale), likely due to the supply of saltier and

345 isotopically heavier seawater from the Southern Adriatic, such as the Levantine Intermediate

346 Water (LIW) that flows northwards in the Adriatic through the Otranto Strait (Stenni *et al.*,

347 1995). $\delta^{13}C_{DIC}$ values also strongly varied along the latitudinal gradient with a range of 3.14‰,

348 compared to the Eastern and Western Mediterranean $\delta^{13}C_{DIC}$ values, 0.41‰ and 0.43‰,

349 respectively (Pierre, 1999). $\delta^{13}C_{DIC}$ increased from North (-0.98‰ in Monfalcone) to South

350 (0.20‰ in Capoiale) with a sharp depleted value in the Po delta area (-2.94‰ in Goro). $\delta^{13}C_{DIC}$

351 along the gradient reflected the contribution of isotopically light carbon from freshwater inflow

352 ($\delta^{13}C_{DIC}$ close to -10.5‰ ± 0.4; Marchina, 2015), from sites around the Po delta.

353

4.2 Shell $\delta^{18}O$

355   Along the latitudinal gradient, temperature and salinity covary and their decrease

356 towards Northern sites led to an $\delta^{18}O_{shell}$ - $\delta^{18}O_{sw}$ increase. Indeed, at thermodynamic

357 equilibrium, $\delta^{18}O_{shell}$ depends on the precipitation temperature and seawater $\delta^{18}O$ (Epstein *et*

358 *al.*, 1951; Craig, 1965; Grossman & Ku, 1986). $\delta^{18}O_{shell}$ - $\delta^{18}O_{sw}$ also reflected differences in $\delta^{18}O$

359 ranging from 0.76‰ in Goro to -1.28‰ in Capoiale. While the site of Goro was close to the

360 expected oxygen isotopic equilibrium (0.77‰), the other five sites showed a negative offset

361 from equilibrium, with the largest offset in Capoiale (-2.05‰). The $\delta^{18}O_{shell}$ - $\delta^{18}O_{sw}$ fluctuation

362 of 2.04‰ between Goro and Capoiale would require temperature variations of about 9°C

363 (Craig, 1965; Grossman & Ku, 1986) if temperatures were the only cause of the $\delta^{18}O_{shell}$ - $\delta^{18}O_{sw}$

364 fluctuation. $\delta^{18}O$ values are also changeable in relation to salinity of the habitat (Craig, 1965)

365 and high fluctuations of salinity in Goro, the site close to Po delta, were likely responsible for

the deviation of temperature derived from measured $\delta^{18}O_{shell}$ - $\delta^{18}O_{sw}$, that didn't reflect the annual fluctuation of seawater temperature. The two Northern sites, Monfalcone and Chioggia, had lower values of $\delta^{18}O_{shell}$ - $\delta^{18}O_{sw}$, suggesting a minor influence of Po freshwater mixing and a contribution of heavier $\delta^{18}O_{sw}$ from the Eastern Adriatic coast.

Temperatures reconstructed from $\delta^{18}O_{shell}$ - $\delta^{18}O_{sw}$ showed that higher SST agreed well with real summer SST, while lower SST was consistently higher than the real winter SST obtained from satellite data. This inconsistency could be attributed to the fact that *C. gallina* precipitates the shell carbonate preferentially during the warm period, while considerably reducing its activity during the cold season (Cespuglio *et al.*, 1999; Keller *et al.*, 2002). The same seasonality of shell growth in the Adriatic Sea was found in the long-lived bivalve *Glycymeris pilosa* and in the venerid *Callista chione* and *Venus verrucosa*, that showed to be a promising archive for the reconstruction of summer seawater temperatures with the slowest growth during winter (Purroy *et al.*, 2018; Peharda *et al.*, 2019; Uvanović *et al.*, 2021). Shell deposition with warm temperatures was reported also for other bivalves from different parts of the globe, such as *Mercenaria stimpsoni*, *Chione cortezi* and *Phacosoma japonicum*, showing that these shells cannot be used as archives of winter temperatures (Tanabe & Oba, 1988; Goodwin *et al.*, 2001; Kubota *et al.*, 2017). In agreement with these previous results, *C. gallina* might be a warm season temperature proxy, suggesting additional complexity in utilizing *C. gallina* shells in paleoclimate studies. Indeed, when shell growth rate is not constant during the year, growth suspensions hamper bivalves from providing uninterrupted records of environmental conditions (Goodwin *et al.*, 2003).

It has been suggested that kinetic effects , associated with the hydration reaction and carbonate biomineralization, during higher calcifications rates increase the relative amount of ^{16}O incorporated in the newly formed shell, resulting in more negative $\delta^{18}O_{shell}$ signatures than equilibrium values (McConnaughey, 1989a). The shells of Southern sites (with higher growth

391 rates; Mancuso *et al.*, 2019), showed the larger oxygen isotopic offset from expected

392 equilibrium, suggesting that together with temperature and salinity, kinetic effects could also

393 explain this observed departure. As bivalves mostly use the oxygen of the ambient water (HCO_3^-

394) rather than ingested food for shell growth (Epstein & Mayeda, 1953; McConnaughey, 1989a),

395 metabolic isotope effects related to respiration can be excluded.

396   From $\delta^{18}O_{shell}$ - $\delta^{18}O_{sw}$ profiles along the *C. gallina* growth direction we could derive

397 considerations on growth rates at the investigated sites in the Adriatic Sea. $\delta^{18}O_{shell}$ - $\delta^{18}O_{sw}$

398 profiles indicated that samples of Cesenatico, San Benedetto and Capoiale were born in spring,

399 while the samples of Monfalcone and Goro, with colder water, were born later in summer. A

400 notable reduction in growth rates with increasing length was also observed in the decreasing

401 amplitude of sinusoidal sequence with clam size. By counting age from seasonal $\delta^{18}O_{shell}$ - $\delta^{18}O_{sw}$

402 peaks, *C. gallina* reached a length of about 20 mm after 1 year in the Southern sites (San

403 Benedetto and Capoiale), and about 13 mm after 1 year in the Northern site (Monfalcone),

404 indicating higher linear extension rates towards the South, in agreement with the previous

405 study (Mancuso *et al.*, 2019).

406

407 **4.3 Shell $\delta^{13}C$**

408 $\delta^{13}C_{shell}$ - $\delta^{13}C_{DIC}$ exhibited a ~1.5‰ range with the largest difference between Goro (0.80‰)

409 and San Benedetto sites (-0.69‰). Seawater $\delta^{13}C_{DIC}$ and metabolic carbon from bivalve

410 respiration and diet significantly affect shell $\delta^{13}C$ values (McConnaughey, 1989b, 1989a;

411 Lorrain *et al.*, 2004; Gillikin *et al.*, 2006). In this study, $\delta^{13}C_{shell}$ - $\delta^{13}C_{DIC}$ was not correlated with

412 latitude, unlike $\delta^{13}C_{DIC}$, implying the contribution of metabolic carbon in *C. gallina* shells.

413 Molluscs shells in coastal areas incorporate carbon from both the riverine and marine

414 reservoirs, so $\delta^{13}C_{shell}$ reflects the mixture (Mook & Vogel, 1968; Gillikin *et al.*, 2006). In this

415 study, the $\delta^{13}C_{shell}$ - $\delta^{13}C_{DIC}$ of *C. gallina* increased with decreasing salinity and increasing

chlorophyll concentration, perhaps as a result of decreasing calcification. *C. gallina* shows

reduced calcification rate with increasing chlorophyll concentration along the same gradient,

perhaps as a result of increased sedimentation as a result of river discharges in proximity to

the Po delta, which could negatively impact the feeding mechanisms of the clams

(McConnaughey & Gillikin, 2008; Pérez *et al.*, 2016; Mancuso *et al.*, 2019).

$\delta^{13}C_{shell}$ - $\delta^{13}C_{DIC}$ profiles along the growth axis showed lower values with increasing length,

more pronounced in the Northern sites, with Goro showing the larger ontogenetic variability

(up to 4.8‰) between the umbo (the older part of shells) and the ventral margin (the youngest

part of shells). In previous studies, the general decreasing trend of $\delta^{13}C$ through ontogeny was

observed to be either caused by the influence of pore water $\delta^{13}C_{DIC}$ gradients, or effects of

metabolic changes (Krantz *et al.*, 1987; Elliot *et al.*, 2003; Lorrain *et al.*, 2004; Gillikin *et al.*,

2007). Indeed, a deeper position in the sediment of older specimens seemed to lead to an

increased supply of ^{13}C depleted pore water produced by the oxidation of organic matter or to

the incorporation of larger amounts of respiratory CO_2 (Keller *et al.*, 2002; Lorrain *et al.*, 2004;

McConnaughey & Gillikin, 2008). Infaunal bivalves may show isotopically depleted values

compared to epifaunal species (Krantz *et al.*, 1987; Keller *et al.*, 2002). Another possible

explanation could be the variation of the metabolism associated with shell growth rates.

Rosenberg and Hughes, 1991 found lower mantle metabolic activity in faster growing shell

portions in *Mytilus edulis*. Lorrain et al., 2004 reported a reduction in the $\delta^{13}C_{shell}$ of *Pecten*

maximus as result of increasing utilization of ^{13}C depleted respiratory CO_2 through ontogeny.

Similarly, higher metabolic rates needed to support carbon requirements for calcification could

explain the decrease of $\delta^{13}C_{shell}$ - $\delta^{13}C_{DIC}$ through ontogeny observed in *C. gallina*. The strong

link between carbon isotopes and bivalve metabolic activity suggests that carbon isotopes are

not reliable indicators of environmental conditions in biogenic carbonates given the high

440 variability of metabolic carbon across seasons, shell growth rates and ontogenetic variations

441 (Lorrain *et al.*, 2004; Geist *et al.*, 2005; Gillikin *et al.*, 2006).

442 *Chamelea gallina* showed a negative offset of 1.9‰ in Goro and 3.4‰ in San Benedetto from

443 the expected carbon isotopic equilibrium (2.7‰), in agreement with most benthic species that

444 generally have depleted $\delta^{13}C$ values compared to carbon isotopic equilibrium (Rau *et al.*, 1982;

445 Keller *et al.*, 2002). The decrease $\delta^{18}O_{shell}$ and $\delta^{13}C_{shell}$ with respect to the equilibrium was in

446 agreement with the classical models driven by kinetic effects, that lead to isotope depleted

447 carbonates (Adkins *et al.*, 2003), highlighting shell stable isotope vital effects in *C. gallina* and

448 contributing to set limits for paleoenvironmental reconstructions for this species.

449

450

451 **5. Conclusions**

452   Bivalve shells can potentially provide information about past estuarine biogeochemical

453 cycles by recording the carbon isotopic signature of dissolved inorganic carbon ($\delta^{13}C_{DIC}$) in

454 estuarine waters. The Adriatic Sea, and especially its Northern basin, plays an important role in

455 carbon cycling being a site of dense water formation during winter and one of the most

456 productive areas in the Mediterranean, contributing to global biogeochemical cycling of carbon

457 and nutrients (Crossland *et al.*, 2005; Catalano *et al.*, 2014). Here we present, for the first time,

458 measurements of shell $\delta^{18}O$ and $\delta^{13}C$ of *C. gallina* combined with seawater $\delta^{18}O$ and $\delta^{13}C_{DIC}$

459 along the 400 km Western Adriatic coasts. The high variability of seawater parameters was

460 expressed in the stable isotopic signature of *C. gallina* along the latitudinal gradient. *Chamelea*

461 *gallina* from Northern sites clearly reflected lower temperature of deposition and the influence

462 of Po river, while shells from Southern sites reflected the salty marine ingressions from the

463 Southern Adriatic. Shells displayed depleted $\delta^{13}C$ values with decreasing salinity and increasing

464 chlorophyll concentration, likely as a result of decreased calcification rates likely due to

465   increased eutrophication and silt and clay of the bottom driven by the river discharges. Almost

466   all specimens exhibited depleted shell $\delta^{18}O$ and $\delta^{13}C$ values compared to the expected isotopic

467   equilibrium. Hence, despite *C. gallina* showing promise as a warm temperature proxy, the large

468   variation in the shell stable isotopic signature points toward noteworthy metabolic and/or

469   kinetic effects in this bivalve, preventing the use of *C. gallina* as a paleoproxy for seawater

470   temperatures.

471

472

REFERENCES

Adkins JF, Boyle EA, Curry WB, Lutringer A (2003) Stable isotopes in deep-sea corals and a new mechanism for "vital effects." *Geochimica et Cosmochimica Acta* **67**, 1129–1143.

Amorosi A, Barbieri G, Bruno L, Campo B, Drexler TM, Hong W, Rossi V, Sammartino I, Scarponi D, Vaiani SC, Bohacs KM (2019) Three-fold nature of coastal progradation during the Holocene eustatic highstand, Po Plain, Italy – close correspondence of stratal character with distribution patterns. *Sedimentology* **66**, 3029–3052.

Bargione G, Vasapollo C, Donato F, Virgili M, Petetta A, Lucchetti A (2020) Age and growth of Striped Venus Clam *Chamelea gallina* (Linnaeus, 1758) in the Mid-Western Adriatic Sea: A comparison of three laboratory techniques. *Frontiers in Marine Science* **7**, 807.

Bemis BE, Geary DH (1996) The usefulness of bivalve stable isotope profiles as environmental indicators: data from the Eastern Pacific Ocean and the Southern Caribbean Sea. *PALAIOS* **11**, 328.

Bemis BE, Spero HJ, Bijma J, Lea DW (1998) Reevaluation of the oxygen isotopic composition of planktonic foraminifera: Experimental results and revised paleotemperature equations. *Paleoceanography* **13**, 150–160.

Böhm F, Joachimski MM, Dullo W-C, Eisenhauer A, Lehnert H, Reitner J, Wörheide G (2000) Oxygen isotope fractionation in marine aragonite of coralline sponges. *Geochimica et Cosmochimica Acta* **64**, 1695–1703.

Bortolami G, Fontes J-CC, Panichi C (1973) Isotopes du milieu et circulations dans les aquiferes du sous-sol Vénitien. *Earth and Planetary Science Letters* **19**, 154–167.

Canuel EA, Cammer SS, McIntosh HA, Pondell CR (2012) Climate Change Impacts on the Organic Carbon Cycle at the Land-Ocean Interface. *Annual Review of Earth and Planetary Sciences* **40**, 685–711.

Catalano G, Azzaro M, Bastianini M, Bellucci LG, Bernardi Aubry F, Bianchi F, Burca M, Cantoni C, Caruso G, Casotti R, Cozzi S, Negro P Del, Fonda Umani S, Giani M, Giuliani S, Kovacevic V, Ferla R La, Langone L, Luchetta A, Monticelli LS, Piacentino S, Pugnetti A, Ravaioli M, Socal G, Spagnoli F, Ursella L (2014) The carbon budget in the northern Adriatic Sea, a winter case study. *Journal of Geophysical Research: Biogeosciences* **119**, 1399–1417.

502   Cespuglio G, Piccinetti C, Longinelli A (1999) Oxygen and carbon isotope profiles from *Nassa*

503   *mutabilis* shells (Gastropoda): accretion rates and biological behaviour. *Marine Biology* **135**,

504   627–634.

505   Chauvaud L, Lorrain A, Dunbar RB, Paulet Y-M, Thouzeau G, Jean F, Guarini J-M, Mucciarone D

506   (2005) Shell of the Great Scallop *Pecten maximus* as a high-frequency archive of

507   paleoenvironmental changes. *Geochemistry, Geophysics, Geosystems* **6**.

508   Cheli A, Mancuso A, Azzarone M, Fermani S, Kaandorp J, Marin F, Montroni D, Polishchuk I,

509   Prada F, Stagioni M (2021) Climate variation during the Holocene influenced the skeletal

510   properties of *Chamelea gallina* shells in the North Adriatic Sea (Italy). *Plos one* **16**, e0247590.

511   Clarke A (1993) Temperature and extinction in the sea: a physiologist's view. *Paleobiology* **19**,

512   499–518.

513   Craig H (1965) The measurement of oxygen isotope paleotemperatures. *Stable isotopes in*

514   *oceanographic studies and paleotemperatures: Consiglio Nazionale delle Richerche* 161–182.

515   Crossland CJ, Kremer HH, Lindeboom H, Crossland JIM, Tissier MDA Le (2005) *Coastal fluxes*

516   *in the Anthropocene: the land-ocean interactions in the coastal zone project of the International*

517   *Geosphere-Biosphere Programme.* Springer Science & Business Media.

518   Degobbis D, Gilmartin M, Revelante N (1986) An annotated nitrogen budget calculation for

519   the northern Adriatic Sea. *Marine Chemistry* **20**, 159–177.

520   Elliot M, DeMenocal PB, Linsley BK, Howe SS (2003) Environmental controls on the stable

521   isotopic composition of *Mercenaria mercenaria*: Potential application to paleoenvironmental

522   studies. *Geochemistry, Geophysics, Geosystems* **4**.

523   Epstein S, Buchsbaum R, Lowenstam H, Urey HC (1951) Carbonate-water isotopic

524   temperature scale. *Geological Society of America Bulletin* **62**, 417–426.

525   Epstein S, Mayeda T (1953) Variation of O^{18} content of waters from natural sources.

526   *Geochimica et Cosmochimica Acta* **4**, 213–224.

527   Feely RA, Sabine CL, Lee K, Berelson W, Kleypas J, Fabry VJ, Millero FJ (2004) Impact of

528   Anthropogenic CO 2 on the CaCO 3 System in the Oceans. *Science* **305**, 362–366.

529   Flora O, Longinelli A (1989) Stable isotope hydrology of a classical karst area, Trieste, Italy. In:

530   *Isotope techniques in the study of the hydrology of fractured and fissured rocks.*

531   Gazeau F, Quiblier C, Jansen JM, Gattuso J-P, Middelburg JJ, Heip CHR (2007) Impact of

532   elevated CO 2 on shellfish calcification. *Geophysical Research Letters* **34**, L07603.

533   Geist J, Auerswald K, Boom A (2005) Stable carbon isotopes in freshwater mussel shells:

534   Environmental record or marker for metabolic activity? *Geochimica et Cosmochimica Acta* **69**,

535   2662–2664.

536   Gillikin DP, Lorrain A, Bouillon S, Willenz P, Dehairs F (2006) Stable carbon isotopic

537   composition of Mytilus edulis shells: relation to metabolism, salinity, $\delta^{13}CDIC$ and

538   phytoplankton. *Organic Geochemistry* **37**, 1371–1382.

539   Gillikin DP, Lorrain A, Meng L, Dehairs F (2007) A large metabolic carbon contribution to the

540    $\delta^{13}C$ record in marine aragonitic bivalve shells. *Geochimica et Cosmochimica Acta* **71**, 2936–

541   2946.

542   Gillikin DP, Ridder F De, Ulens H, Elskens M, Keppens E, Baeyens W, Dehairs F (2005)

543   Assessing the reproducibility and reliability of estuarine bivalve shells (*Saxidomus giganteus*)

544   for sea surface temperature reconstruction: implications for paleoclimate studies.

545   *Palaeogeography, Palaeoclimatology, Palaeoecology* **228**, 70–85.

546   Gilmartin M, Degobbis D, Revelante N, Smodlaka N (1990) The mechanism controlling plant

547   nutrient concentrations in the northern Adriatic Sea. *Internationale Revue der gesamten*

548   *Hydrobiologie und Hydrographie* **75**, 425–445.

549   Giordani P, Helder W, Koning E, Miserocchi S, Danovaro R, Malaguti A (2002) Gradients of

550   benthic–pelagic coupling and carbon budgets in the Adriatic and Northern Ionian Sea. *Journal*

551   *of Marine Systems* **33**, 365–387.

552   Gizzi F, Caccia MG, Simoncini GA, Mancuso A, Reggi M, Fermani S, Brizi L, Fantazzini P,

553   Stagioni M, Falini G, Piccinetti C, Goffredo S (2016) Shell properties of commercial clam

554   Chamelea gallina are influenced by temperature and solar radiation along a wide latitudinal

555   gradient. *Scientific Reports* **6**, 36420.

556   Goodwin DH, Flessa KW, Schone BR, Dettman DL (2001) Cross-calibration of daily growth

557   increments, stable isotope variation, and temperature in the Gulf of California bivalve mollusk

558   *Chione cortezi*: implications for paleoenvironmental analysis. *PALAIOS* **16**, 387–398.

559   Goodwin DH, Schone BR, Dwttman DL (2003) Resolution and fidelity of oxygen isotopes as

560   paleotemperature proxies in bivalve mollusk shells: models and observations. *PALAIOS* **18**,

561   110–125.

562   Grossman EL, Ku T-LL (1986) Oxygen and carbon isotope fractionation in biogenic aragonite:

563   Temperature effects **59**, 59–74.

564   Hall-Spencer JM, Harvey BP (2019) Ocean acidification impacts on coastal ecosystem services

565   due to habitat degradation. *Emerging Topics in Life Sciences* **3**, 197–206.

566   Harris KE, DeGrandpre MD, Hales B (2013) Aragonite saturation state dynamics in a coastal

567   upwelling zone. *Geophysical Research Letters* **40**, 2720–2725.

568   Hickson JA, Johnson AL., Heaton TH., Balson PS (1999) The shell of the Queen Scallop

569   *Aequipecten opercularis* (L.) as a promising tool for palaeoenvironmental reconstruction:

570   Evidence and reasons for equilibrium stable-isotope incorporation. *Palaeogeography,*

571   *Palaeoclimatology, Palaeoecology* **154**, 325–337.

572   Jones PD, Briffa KR, Osborn TJ, Lough JM, Ommen TD van, Vinther BM, Luterbacher J, Wahl ER,

573   Zwiers FW, Mann ME, Schmidt GA, Ammann CM, Buckley BM, Cobb KM, Esper J, Goosse H,

574   Graham N, Jansen E, Kiefer T, Kull C, Küttel M, Mosley-Thompson E, Overpeck JT, Riedwyl N,

575   Schulz M, Tudhope AW, Villalba R, Wanner H, Wolff E, Xoplaki E (2009) High-resolution

576   palaeoclimatology of the last millennium: a review of current status and future prospects. *The*

577   *Holocene* **19**, 3–49.

578   Keller N, Piero D Del, Longinelli A (2002) Isotopic composition, growth rates and biological

579   behaviour of *Chamelea gallina* and *Callista chione* from the Gulf of Trieste (Italy). *Marine*

580   *Biology* **140**, 9–15.

581   Klein RT, Lohmann KC, Thayer CW (1996a) Bivalve skeletons record sea-surface temperature

582   and $\delta^{18}O$ via Mg/Ca and $^{18}O/^{16}O$ ratios. *Geology* **24**, 415–418.

583   Klein RT, Lohmann KC, Thayer CW (1996b) Sr Ca and $^{13}C^{12}C$ ratios in skeletal calcite of

584   Mytilus trossulus: Covariation with metabolic rate, salinity, and carbon isotopic composition

585   of seawater. *Geochimica et Cosmochimica Acta* **60**, 4207–4221.

586   Krantz DE, Williams DF, Jones DS (1987) Ecological and paleoenvironmental information
587   using stable isotope profiles from living and fossil molluscs. *Palaeogeography,*
588   *Palaeoclimatology, Palaeoecology* **58**, 249–266.

589   Kubota K, Shirai K, Murakami-Sugihara N, Seike K, Hori M, Tanabe K (2017) Annual shell
590   growth pattern of the Stimpson's hard clam *Mercenaria stimpsoni* as revealed by
591   sclerochronological and oxygen stable isotope measurements. *Palaeogeography,*
592   *Palaeoclimatology, Palaeoecology* **465**, 307–315.

593   Leng MJ, Lewis JP (2016) Oxygen isotopes in Molluscan shell: Applications in environmental
594   archaeology. *Environmental Archaeology* **21**, 295–306.

595   Lorrain A, Paulet Y-M, Chauvaud L, Dunbar R, Mucciarone D, Fontugne M (2004) $\delta^{13}C$
596   variation in scallop shells: Increasing metabolic carbon contribution with body size?
597   *Geochimica et Cosmochimica Acta* **68**, 3509–3519.

598   Mancuso A, Stagioni M, Prada F, Scarponi D, Piccinetti C, Goffredo S (2019) Environmental
599   influence on calcification of the bivalve *Chamelea gallina* along a latitudinal gradient in the
600   Adriatic Sea. *Scientific Reports* **9**, 11198.

601   Marchina C (2015) Geochemical and isotopic investigation on the Po river waters from
602   Monviso sources to its delta: natural and anthropogenic components. *Unpublished Ph.D. thesis,*
603   *University of Ferrara*.

604   Matozzo V, Monari M, Foschi J, Serrazanetti GP, Cattani O, Marin MG (2007) Effects of salinity
605   on the clam *Chamelea gallina*. Part I: alterations in immune responses. *Marine Biology* **151**,
606   1051–1058.

607   McConnaughey T (1989a) ^{13}C and ^{18}O isotopic disequilibrium in biological carbonates: II. In
608   vitro simulation of kinetic isotope effects. *Geochimica et Cosmochimica Acta* **53**, 163–171.

609   McConnaughey T (1989b) ^{13}C and ^{18}O isotopic disequilibrium in biological carbonates: I.
610   Patterns. *Geochimica et Cosmochimica Acta* **53**, 151–162.

611   McConnaughey TA, Burdett J, Whelan JF, Paull CK (1997) Carbon isotopes in biological
612   carbonates: Respiration and photosynthesis. *Geochimica et Cosmochimica Acta* **61**, 611–622.

613   McConnaughey TA, Gillikin DP (2008) Carbon isotopes in mollusk shell carbonates. *Geo-*

614   *Marine Letters* **28**, 287–299.

615   Monari M, Matozzo V, Foschi J, Cattani O, Serrazanetti GP, Marin MG (2007a) Effects of high
616   temperatures on functional responses of haemocytes in the clam *Chamelea gallina*. *Fish and*
617   *Shellfish Immunology*.

618   Monari M, Serrazanetti GP, Foschi J, Matozzo V, Marin MG, Cattani O (2007b) Effects of salinity
619   on the clam *Chamelea gallina* haemocytes. Part II: Superoxide dismutase response. *Marine*
620   *Biology*.

621   Montanari A (2012) Hydrology of the Po River: looking for changing patterns in river
622   discharge. *Hydrology and Earth System Sciences* **16**, 3739–3747.

623   Mook WG, Vogel JC (1968) Isotopic equilibrium between shells and their environment. *Science*
624   **159**, 874–875.

625   Peharda M, Vilibić I, Black B, Uvanović H, Markulin K, Mihanović H (2019) A network of
626   bivalve chronologies from semi-enclosed seas. *Plos one* **14**, e0220520.

627   Pérez CA, Lagos NA, Saldías GS, Waldbusser G, Vargas CA (2016) Riverine discharges impact
628   physiological traits and carbon sources for shell carbonate in the marine intertidal mussel
629   *Perumytilus purpuratus*. *Limnology and Oceanography* **61**, 969–983.

630   Pettine M, Patrolecco L, Camusso M, Crescenzio S (1998) Transport of carbon and nitrogen to
631   the northern Adriatic Sea by the Po River. *Estuarine, Coastal and Shelf Science* **46**, 127–142.

632   Pierre C (1999) The oxygen and carbon isotope distribution in the Mediterranean water
633   masses. *Marine Geology* **153**, 41–55.

634   Prada F, Yam R, Levy O, Caroselli E, Falini G, Dubinsky Z, Goffredo S, Shemesh A (2019) Kinetic
635   and metabolic isotope effects in zooxanthellate and non-zooxanthellate Mediterranean corals
636   along a wide latitudinal gradient. *Frontiers in Marine Science* **6**, 522.

637   Purroy A, Milano S, Schöne BR, Thébault J, Peharda M (2018) Drivers of shell growth of the
638   bivalve, *Callista chione* (L. 1758) – Combined environmental and biological factors. *Marine*
639   *Environmental Research* **134**, 138–149.

640   Raicich F (1996) On the fresh balance of the Adriatic Sea. *Journal of Marine Systems* **9**, 305–

641   319.

642   Rau GH, Sweeney RE, Kaplan IR (1982) Plankton ^{13}C:^{12}C ratio changes with latitude:

643   differences between northern and southern oceans. *Deep Sea Research Part A, Oceanographic*

644   *Research Papers*.

645   Regnier P, Friedlingstein P, Ciais P, Mackenzie FT, Gruber N, Janssens IA, Laruelle GG,

646   Lauerwald R, Luyssaert S, Andersson AJ, Arndt S, Arnosti C, Borges A V., Dale AW, Gallego-Sala

647   A, Goddéris Y, Goossens N, Hartmann J, Heinze C, Ilyina T, Joos F, LaRowe DE, Leifeld J,

648   Meysman FJR, Munhoven G, Raymond PA, Spahni R, Suntharalingam P, Thullner M (2013)

649   Anthropogenic perturbation of the carbon fluxes from land to ocean. *Nature Geoscience* **6**,

650   597–607.

651   Rhoads D, Lutz R (1980) Skeletal growth of aquatic organisms: biological records of

652   environmental change.

653   Richardson CA (2001) Molluscs as archives of environmental change.

654   Ridente D, Foglini F, Minisini D, Trincardi F, Verdicchio G (2007) Shelf-edge erosion, sediment

655   failure and inception of Bari Canyon on the Southwestern Adriatic Margin (Central

656   Mediterranean). *Marine Geology* **246**, 193–207.

657   Ridente D, Trincardi F, Piva A, Asioli A, Cattaneo A (2008) Sedimentary response to climate

658   and sea level changes during the past~ 400 ka from borehole PRAD1–2 (Adriatic margin).

659   *Geochemistry, Geophysics, Geosystems* **9**.

660   Romanek CS, Grossman EL, Morse JW (1992) Carbon isotopic fractionation in synthetic

661   aragonite and calcite: Effects of temperature and precipitation rate. *Geochimica et*

662   *Cosmochimica Acta* **56**, 419–430.

663   Rosenberg GD, Hughe WW (1991) A metabolic model for the determination of shell

664   composition in the bivalve mollusc, *Mytilus edulis*. *Lethaia* **24**, 83–96.

665   RStudio Team (2020) RStudio: Integrated Development for R. RStudio, PBC, Boston, MA URL

666   http://www.rstudio.com/.

667   Russo A, Artegiani A (1996) Adriatic sea hydrography. *Scientia Marina* **60**, 33–43.

668   Sadler J, Carré M, Azzoug M, Schauer AJ, Ledesma J, Cardenas F, Chase BM, Bentaleb I, Muller

669   SD, Mandeng M, Rohling EJ, Sachs JP (2012) Reconstructing past upwelling intensity and the

670   seasonal dynamics of primary productivity along the Peruvian coastline from mollusk shell

671   stable isotopes. *Geochemistry, Geophysics, Geosystems* **13**, n/a-n/a.

672   Salisbury J, Green M, Hunt C, Campbell J (2008) Coastal acidification by rivers: a threat to

673   shellfish? *Eos, Transactions American Geophysical Union* **89**, 513–513.

674   Schöne B, Tanabe K, Dettman D, Sato S (2003) Environmental controls on shell growth rates

675   and $\delta^{18}O$ of the shallow-marine bivalve mollusk *Phacosoma japonicum* in Japan. *Marine*

676   *Biology* **142**, 473–485.

677   Schöne BR (2008) The curse of physiology—challenges and opportunities in the

678   interpretation of geochemical data from mollusk shells. *Geo-Marine Letters* **28**, 269–285.

679   Schöne BR, Gillikin DP (2013) Unraveling environmental histories from skeletal diaries —

680   Advances in sclerochronology. *Palaeogeography, Palaeoclimatology, Palaeoecology* **373**, 1–5.

681   Spero HJ, Bijma J, Lea DW, Bemis BE (1997) Effect of seawater carbonate concentration on

682   foraminiferal carbon and oxygen isotopes. *Nature* **390**, 497–500.

683   Stenni B, Nichetto P, Bregant D, Scarazzato P, Longinelli A (1995) The Delta-O-18 signal of the

684   northward flow of mediterranean waters in the Adriatic Sea. *Oceanologica acta* **18**, 319–328.

685   Tanabe K, Oba T (1988) Latitudinal variation in shell growth patterns of *Phacosoma*

686   *japonicum* (Bivalvia: Veneridae) from the Japanese coast. *Marine Ecology Progress Series* 75–

687   82.

688   Tanaka N, Monaghan MC, Rye DM (1986) Contribution of metabolic carbon to mollusc and

689   barnacle shell carbonate. *Nature* **320**, 520–523.

690   Tesi T, Miserocchi S, Goni MA e a1, Langone L, Boldrin A, Turchetto M (2007) Organic matter

691   origin and distribution in suspended particulate materials and surficial sediments from the

692   western Adriatic Sea (Italy). *Estuarine, Coastal and Shelf Science* **73**, 431–446.

693   Tripati AK, Eagle RA, Thiagarajan N, Gagnon AC, Bauch H, Halloran PR, Eiler JM (2010) $^{13}C–^{18}O$

694   isotope signatures and 'clumped isotope' thermometry in foraminifera and coccoliths.

695   *Geochimica et Cosmochimica Acta* **74**, 5697–5717.

696   Urey HC (1948) Oxygen Isotopes in Nature and in the Laboratory. *New Series* **108**, 489–496.

697   Uvanović H, Schöne BR, Markulin K, Janeković I, Peharda M (2021) Venerid bivalve *Venus*
698   *verrucosa* as a high-resolution archive of seawater temperature in the Mediterranean Sea.
699   *Palaeogeography, Palaeoclimatology, Palaeoecology* **561**, 110057.

700   Vihtakari M, Ambrose WG, Renaud PE, Locke WL, Carroll ML, Berge J, Clarke LJ, Cottier F, Hop
701   H (2017) A key to the past? Element ratios as environmental proxies in two Arctic bivalves.
702   *Palaeogeography, Palaeoclimatology, Palaeoecology* **465**, 316–332.

703   Wefer G, Berger WH (1991) Isotope paleontology: growth and composition of extant
704   calcareous species. *Marine Geology* **100**, 207–248.

705   Wheeler A (1992) Mechanisms of molluscan shell formation. *Calcification in Biological*
706   *Systems*.

707   Zavatarelli M, Raicich F, Bregant D, Russo A, Artegiani A (1998) Climatological biogeochemical
708   characteristics of the Adriatic Sea. *Journal of Marine Systems* **18**, 227–263.

709   Zeebe RE (1999) An explanation of the effect of seawater carbonate concentration on
710   foraminiferal oxygen isotopes. *Geochimica et Cosmochimica Acta* **63**, 2001–2007.

711

712   **TABLES**
713
714   **Table 1. Seawater Isotope data.** $\delta^{18}O_{sw}$ (summer, winter and annual average seawater) and

715    $\delta^{13}C_{DIC}$ (summer, winter and annual average seawater). Values for each site in decreasing

716   order of latitude: MO (Monfalcone), CH (Chioggia), GO (Goro), CE (Cesenatico), SB (San

717   Benedetto), CA (Capoiale). K-W, Kruskal-Wallis test; *** $p<0.001$.

Site	Latitude (°)	Summer $\delta^{18}O_{sw}$	Winter $\delta^{18}O_{sw}$	Annual mean $\delta^{18}O_{sw}$	Summer $\delta^{13}C_{DIC}$	Winter $\delta^{13}C_{DIC}$	Annual mean $\delta^{13}C_{DIC}$
MO	45.70	0.80	0.12	0.46	-0.05	-1.91	-0.98
CH	45.20	-1.24	0.87	-0.19	-0.73	-0.79	-0.76
GO	44.78	-2.84	-0.65	-1.75	-3.54	-2.34	-2.94
CE	44.18	0.47	-0.60	-0.06	-1.56	-1.88	-1.72
SB	43.08	1.32	0.68	1.00	-0.21	-0.79	-0.50
CA	41.92	1.63	1.41	1.52	0.28	0.11	0.20
K-W		***	***	***	***	***	***

Table 2. Shell Isotope data. SE, standard error of the shell isotope values for each site. KW, Kruskal-Wallis test; *** p<0.001. Values for each site in decreasing order of latitude: MO (Monfalcone), CH (Chioggia), GO (Goro), CE (Cesenatico), SB (San Benedetto), CA (Capoiale).

Site	n	$\delta^{18}O_{shell}$ (SE)	$\delta^{18}O_{shell}$ - $\delta^{18}O_{sw}$	$\delta^{13}C_{shell}$ (SE)	$\delta^{13}C_{shell}$ - $\delta^{13}C_{DIC}$
MO	8	-0.31 (0.12)	-0.76	-1.47 (0.11)	-0.49
CH	7	-0.83 (0.04)	-0.64	-1.16 (0.10)	-0.40
GO	7	-0.98 (0.20)	0.76	-2.14 (0.15)	0.80
CE	7	-0.91 (0.16)	-0.85	-1.62 (0.11)	0.10
SB	7	-0.08 (0.11)	-1.08	-1.20 (0.09)	-0.69
CA	7	0.24 (0.08)	-1.28	-0.34 (0.05)	-0.54
K-W		***	***	***	***

a.

MO

CH

GO

CE

Adriatic Sea

SB

CA

N

100 km

b

Site	Code	Latitude (°)
Monfalcone	MO	45.7
Chioggia	CH	45.2
Goro	GO	44.8
Cesenatico	CE	44.2
San Benedetto	SB	43.1
Capoiale	CA	41.9

c

Code	n	SST (°C) mean (SE)	SSS (PSU) mean (SE)
MO	1447	16.96 (0.19)	35.43 (0.03)
CH	1447	16.47 (0.19)	30.89 (0.09)
GO	1447	16.54 (0.19)	28.52 (0.08)
CE	1447	17.05 (0.20)	34.19 (0.04)
SB	1447	17.90 (0.19)	36.29 (0.03)
CA	1447	18.60 (0.17)	37.43 (0.01)

d

Code	n	CHL (mg/m^3) mean (SE)
MO	48	4.5 (0.20)
CH	48	2.88 (0.22)
GO	48	4.98 (0.38)
CE	48	6.23 (0.59)
SB	48	2.09 (0.27)
CA	48	1.21 (0.18)

Figure 1. Map of the Adriatic Sea and environmental parameters.

a. Adriatic coastline with sampling sites of C. gallina clams. Po river labelled with green lines. Abbreviations and coordinates of the sites in decreasing order of latitude: MO, Monfalcone 45°42'N, 13°14'E; CH, Chioggia 45°12'N, 12°19'E; GO, Goro 44°47'N, 12°25'E; CE, Cesenatico 44°11'N, 12°26'E; SB, San Benedetto 43°5'N, 13°51'E; CA, Capoiale 41°55'N, 15°39'E. The map was downloaded from d-maps.com site (http://www.d-maps.com) and modified with Adobe Photoshop CS4. b-c-d. Latitude, annual average values for sea surface temperature (SST), sea surface salinity (SSS) and chlorophyll concentration (CHL) from 2011 to 2015. n = number of collected data, daily data for SST and SSS and monthly data for CHL; SE = standard error.
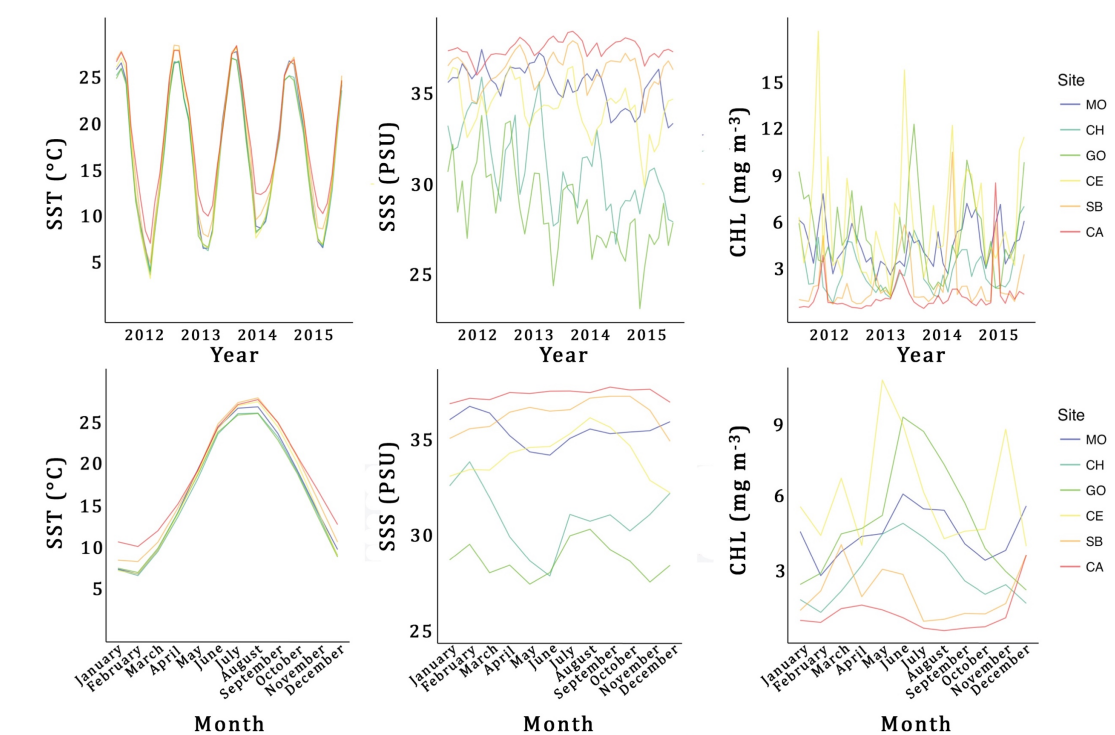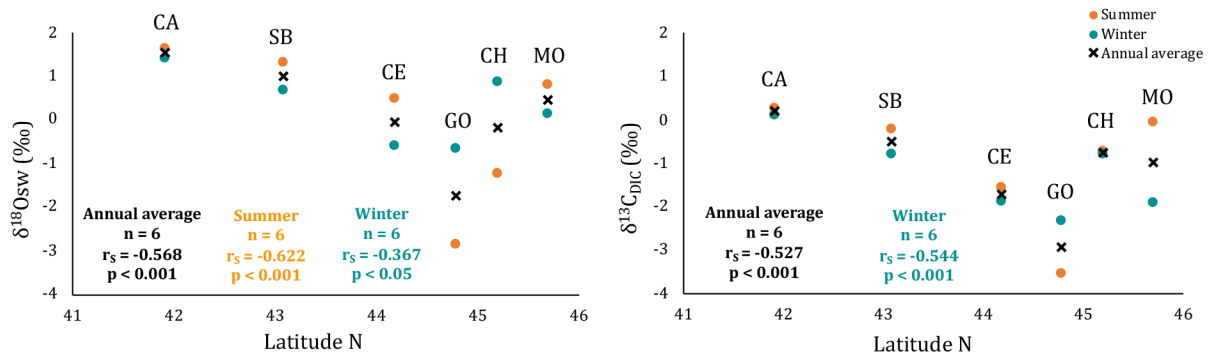
728

Figure 2. Inter-annual and intra-annual variations of SST, SSS and CHL among sites.
Inter-annual data from July 2011 to June 2015. Intra-annual data are the mean monthly
values of four years. Abbreviations in decreasing order of latitude: MO, Monfalcone; CH,
Chioggia; GO, Goro; CE, Cesenatico; SB, San Benedetto; CA, Capoiale.

732

733

734

Figure 3. The relation between summer, winter and annual mean $\delta^{18}O_{sw}$ and $\delta^{13}C_{DIC}$ with latitude in six sites along the Western coast of the Adriatic Sea (~400 km transect). Orange dots are summer values, green dots are the winter ones and black crosses are the annual isotope average between summer and winter. No statistics included for summer $\delta^{13}C_{DIC}$ because of lack of statistically significant. MO, Monfalcone; CH, Chioggia; GO, Goro; CE, Cesenatico; SB, San Benedetto; CA, Capoiale.

741

742
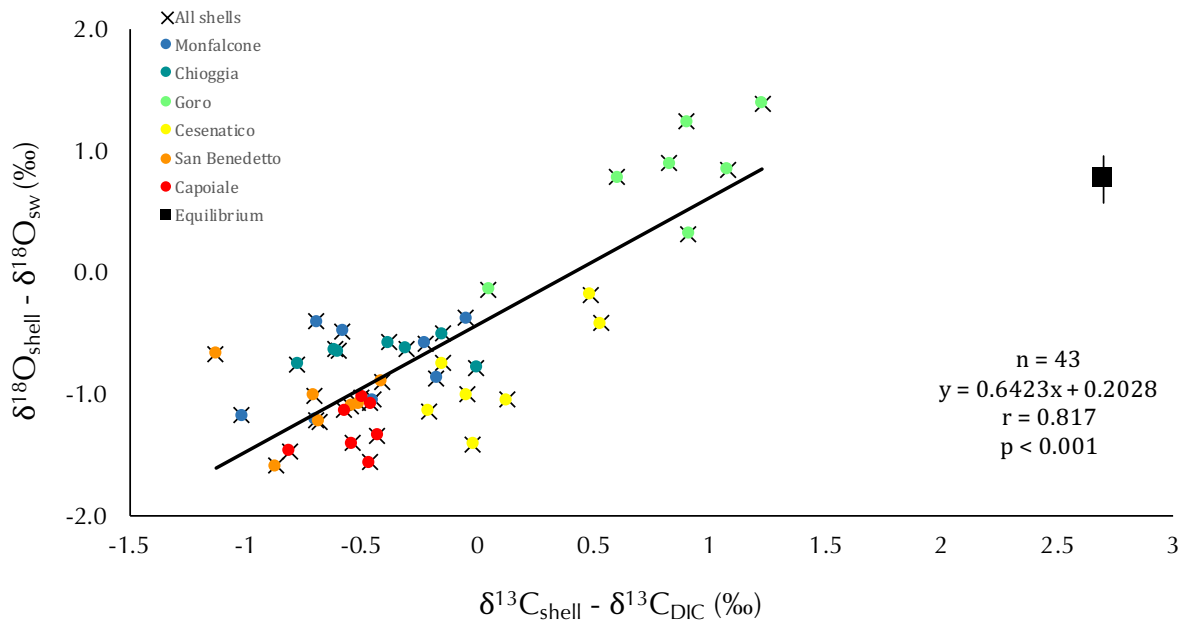
Figure 4. Isotopic comparison among the six sites along the Adriatic coasts of Italy. The black square depicts the mean estimated aragonite equilibrium value among sites, and the

vertical line shows the range of equilibrium values related to local maximum and minimum

temperature along the gradient.
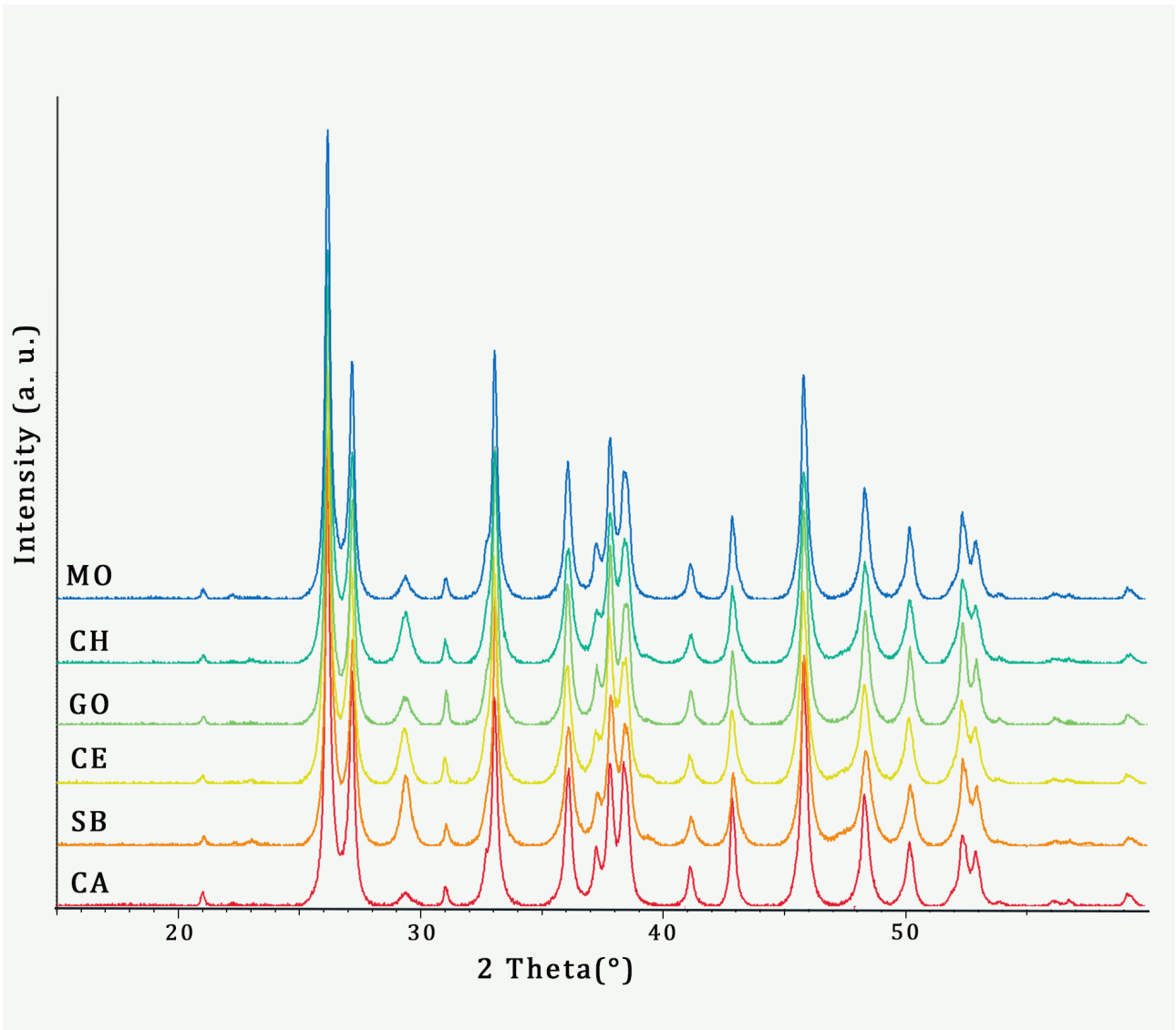
Figure 5. X-ray powder diffraction (XRD) patterns from ground shells of *C. gallina*. A diffraction pattern is shown for each site. All the peaks were assigned to aragonite.
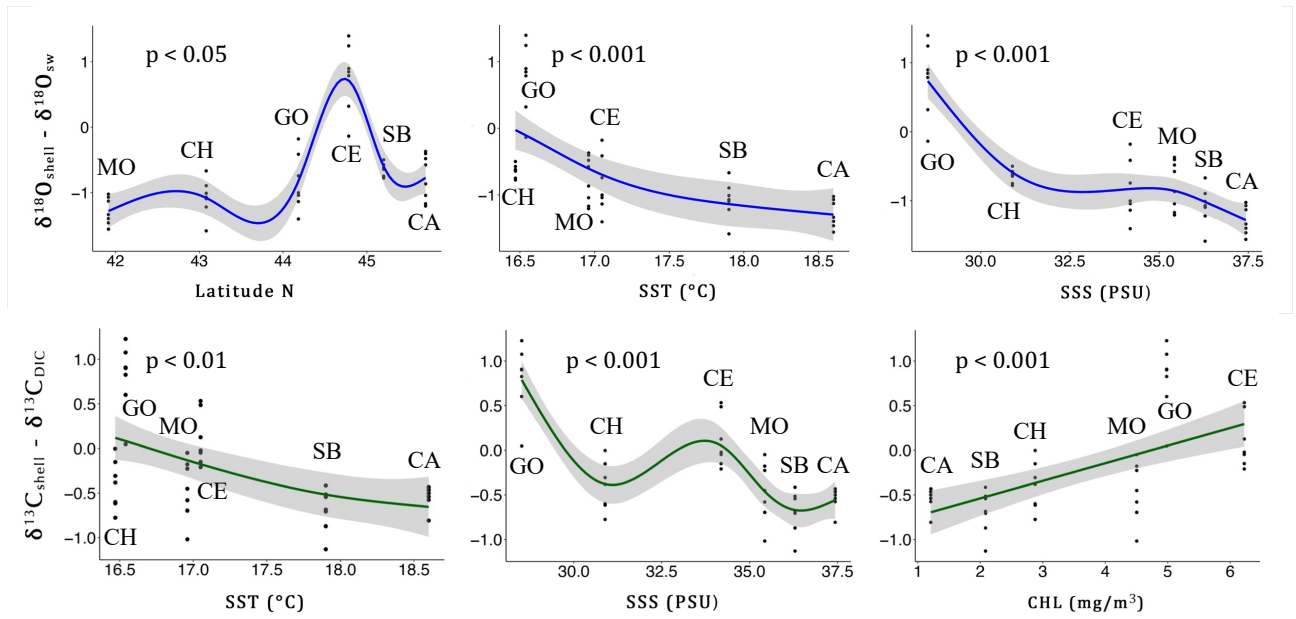
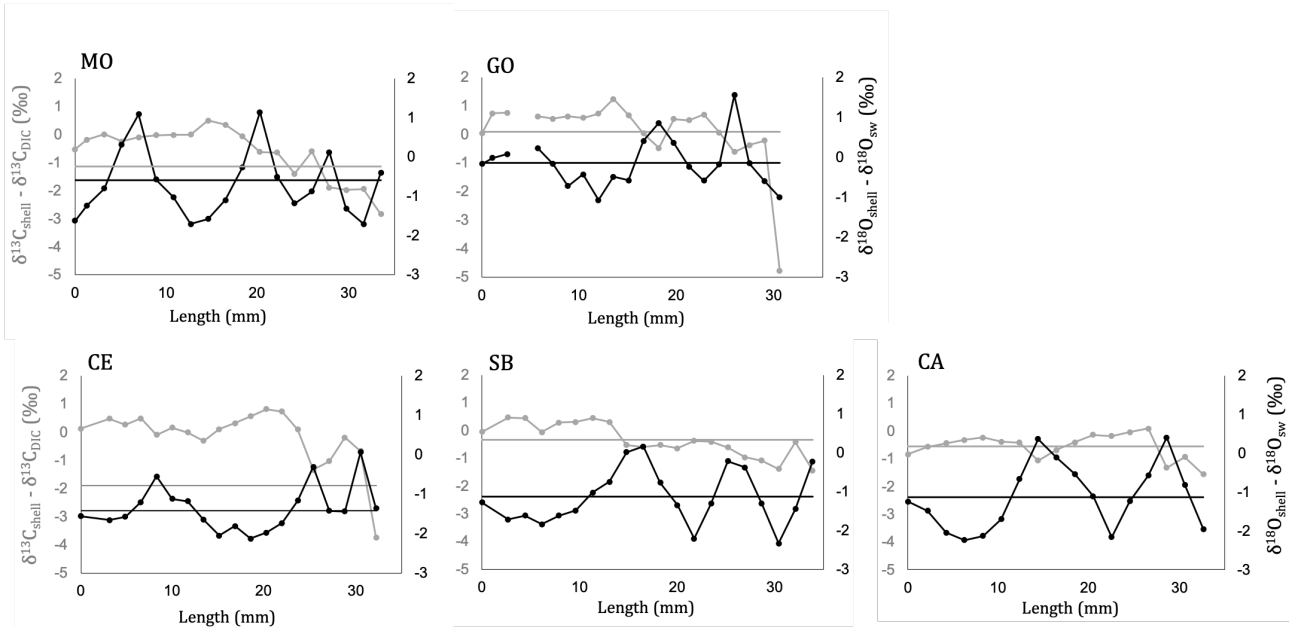**Figure 6. Estimated smooth curve from GAM models.** Scatterplots of $\delta^{18}O_{shell}$ - $\delta^{18}O_{sw}$ and

$\delta^{13}C_{shell}$ - $\delta^{13}C_{DIC}$ with fitted smooth terms s(Lat), s(SST), s(SSS), s(CHL) (solid line). Number of

degrees of freedom=*6* and 95% confidence intervals (grey shade). See Table 3 for statistics.

761

Figure 7. δ¹⁸O$_{shell}$ - δ¹⁸O$_{sw}$ and δ¹³C$_{shell}$ - δ¹³C$_{DIC}$ **profiles along the shell growth axis**. Grey lines represent δ¹³C, black lines are δ¹⁸O and points on the lines are the drilled spots. The lower values indicate summer, while the higher values indicate winter. The average values of the drilled spots at each site are reported as horizontal line. No seasonal data for Chioggia.
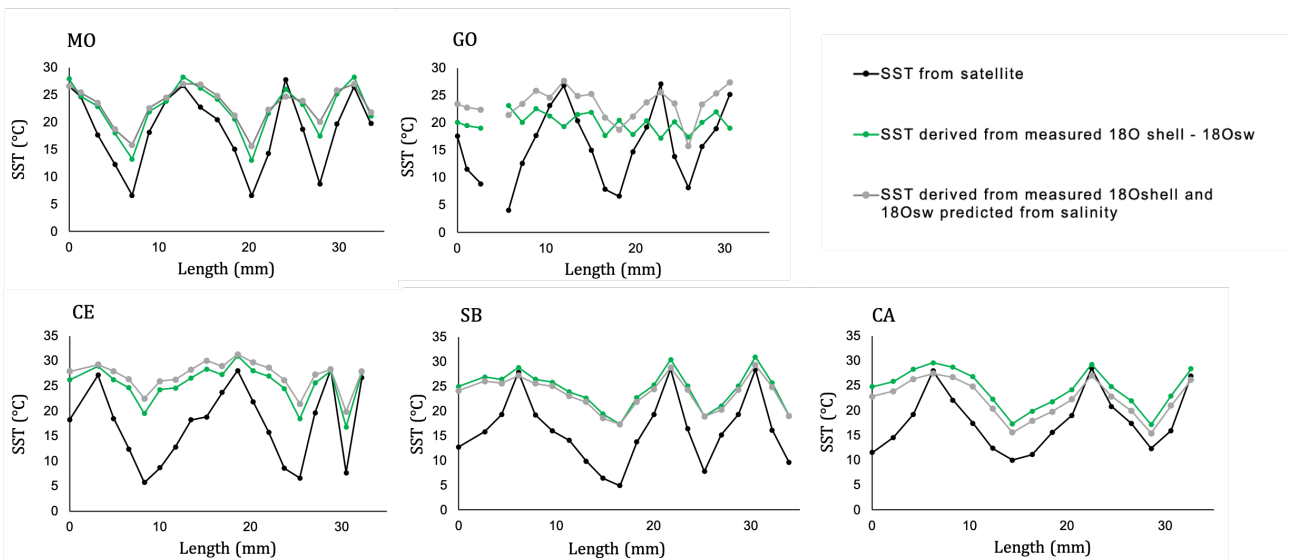

Figure 8. Comparison between SST from satellite and derived SST from oxygen isotopes of *C. gallina*. SST derived from δ¹⁸O$_{shell}$ along shell growth axis and measured δ¹⁸O$_{sw}$ (green line) and predicted δ¹⁸O$_{sw}$ (grey line), using the equation from Grossman and Ku,

772   1986(Grossman & Ku, 1986) [T = 20.6 – 4.34($\delta^{18}O_{arag}$ – ($\delta^{18}O_{sw}$ - 0.27))]. Winter, summer or

773   average $\delta^{18}O_{sw}$ were considered depending on seasonal profile observed in the sinusoidal

774   sequence of oxygen isotopes during shell growth. Predicted $\delta^{18}O_{sw}$ was calculated from salinity

775   data (grey line) using the equation derived from Purroy *et al.*, 2018 [$\delta^{18}O_{sw}$ = 0.23 x salinity -

776   7.54]. Winter, summer or average salinity SST obtained from satellite data (balck line).

777
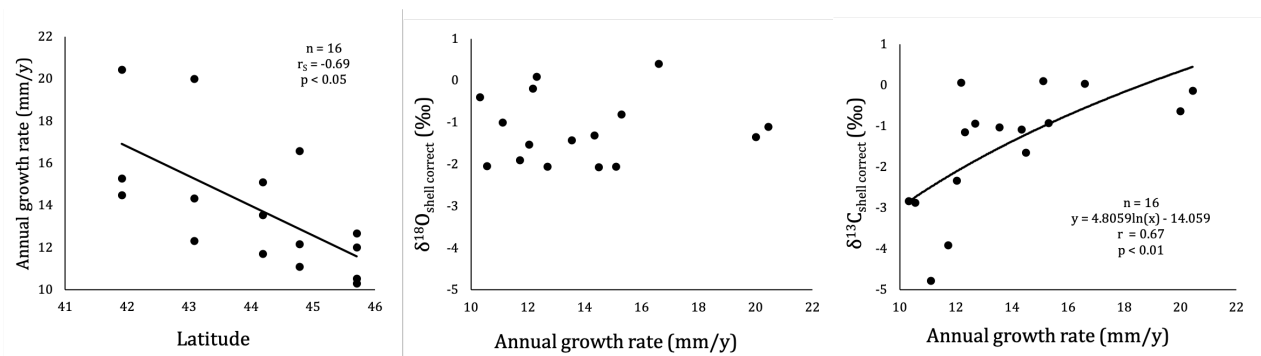
778   **Figure 9. Relationship between annual growth rates with latitude, $\delta^{18}O_{shell}$ - $\delta^{18}O_{sw}$ and**

779   **$\delta^{13}C_{shell}$ - $\delta^{13}C_{DIC}$.** Growth rates are calculated from the length-age key at each year, by means of

780    $\delta^{18}O$ profile along the shell growth axis.

781

782

783